



Transition from covalent to metallic behavior in group-14 clusters

Alexandre A. Shvartsburg, Martin F. Jarrold *

Department of Chemistry, Northwestern University, 2145 Sheridan Road, Evanston, IL 60208-3113, USA

Received 2 September 1999; in final form 6 December 1999

Abstract

We have probed the structures of Pb_n cations up to $n = 32$ using ion mobility measurements. These species assume compact near-spherical morphologies for all sizes studied. This behavior is characteristic of clusters of the metallic elements. Silicon, germanium, and tin clusters in the same size range have previously been found to adopt prolate geometries produced by stacking tricapped trigonal prism units. So the transition to ‘normal’ metal cluster growth in the group-14 elements occurs between tin and lead, one row lower than the transition from covalent to metallic bonding in the bulk solids under ambient conditions. © 2000 Elsevier Science B.V. All rights reserved.

1. Introduction

Some metals, such as alkaline earths [1] and certain transition metals [2], yield clusters with geometric shell structures, where atoms are arranged in an ordered packing of hard spheres. Clusters of free electron metals such as alkali [1], coinage [1], and group-13 elements [1,3–5] normally adopt the electronic shell structure. This means that the atoms conform to the arrangement minimizing total electronic energy. Species of the group-12 elements undergo a transition from geometric to electronic shell structure once the s- and p-electronic bands are hybridized, which allows electronic delocalization [6]. Eventually, all clusters must assume the geometric shell structure of the solid bulk element. Summarizing, metal clusters, whether governed by electronic or by geometric shell structure, grow as densely

packed objects without major deviations from spherical shape.

Conversely, clusters of covalently bound non-metals usually have more open geometries that satisfy the specific highly-directional bonding requirements of these elements. For example, S and Se clusters adopt chain and ring geometries [7,8] while B_n species supposedly exist as quasiplanar sheets [9]. Clusters of group-14 elements: carbon [10], silicon [11], and germanium [12] have received the greatest attention. Carbon species may assume geometries as diverse as chains, rings, graphite sheets, and fullerenes [10,13,14]. Si and Ge clusters form prolate structures up to $n \approx 25$ –35, but then rearrange to more spherical morphologies [11,12]. The prolate sequences for Si_n or Ge_n are built by stacking exceptionally stable Si_9 or Ge_9 tricapped trigonal prism (TTP) units [15–17]. Recently we found [18] that Sn_n cations in the $n \leq 35$ range adopt the same type of ‘stacked TTP’ prolate morphologies, although the geometries differ from those of either

* Corresponding author. Fax: +1-847-491-7713; e-mail: mfj@nwu.edu

Ge_n^+ or Si_n^+ in details. This was unexpected, because the normal allotrope of tin under ambient conditions (white tin) is a typical metal. No metallic element has previously been found to produce clusters with highly non-compact geometries appropriate for covalently bound species. In a sense, the covalent-to-metallic transition that occurs between the fourth and fifth row of the Periodic Table for group-14 elements in the bulk fails to occur in their clusters. Then a natural question to ask is whether this transition occurs for lead clusters.

The major features in the abundance distributions for Pb_n cations are maxima ('magic numbers') at $n = 7, 10, 13,$ and 19 and a deep minimum at $n = 14$ [19–23]. These had been explained assuming an icosahedral growth, where $n = 7, 13,$ and 19 correspond to particularly stable geometric shells (however, $n = 10$ is not special with icosahedral packing) [19–24]. The abundance distributions for $\text{Si}_n^+, \text{Ge}_n^+$, and Sn_n^+ often peak at different n , primarily 4 and 6 [25]. On the basis of this, it had been deduced that the transition from covalent to metallic bonding in group-14 elements occurs between tin and lead. However, the magic numbers are determined by both thermodynamic and kinetic factors, and often depend on the source design and mode of operation. For example, the abundance distributions of Pb_n^+ ejected from a liquid metal ion source are featureless [25]. Furthermore, the mass spectra of Sn_n^+ produced under different conditions resemble those of Pb_n^+ closer than those of Si_n^+ and Ge_n^+ [21,26]. These results led to the conclusion that tin clusters are 'metallic' like lead ones rather than covalently bound like Si_n^+ and Ge_n^+ , and that the transition to metallic bonding occurs for tin clusters. Further, the magic numbers for Pb_n^- and Pb_n^+ are not the same [27,28], while Pb_n^{++} exhibit the abundance distribution appropriate for electronic, rather than geometric shell structure [29]. The electron affinities of Pb_n anions [27,28] overall follow the jellium model [28], which suggests metallic bonding. However, the agreement is not as good [28] as that for clusters of other metals. The reactivities of Pb_n^+ [30] and Pb_n^- [31] versus $\text{O}_2, \text{NO},$ and NO_2 have been measured, but this yielded no hints as to the structure.

A few calculations have been performed for lead clusters. Dai and Balasubramanian investigated $\text{Pb}_4, \text{Pb}_4^+,$ and Pb_5 [33]. Pb_n neutrals and anions with

$n \leq 10$ were optimized by density functional theory [34]. These studies have revealed no differences between the geometries of tin and lead species for any size or charge state. Semiempirical calculations [35] suggested that larger ($n \approx 15\text{--}50$) Pb clusters may have both prolate and near-spherical shapes.

2. Ion mobility in Pb_n^+ ($n \leq 32$) cations

In this Letter we report on the mobility measurements for singly charged Pb_n ($n \leq 32$) cations. The tandem quadrupole drift tube instrument employed in this work has been described previously [3]. Briefly, the cluster ions are generated by pulsed 308 nm laser vaporization of a translated and rotated lead rod (Alfa Aesar) and entrained in a continuous helium flow. They are mass selected and injected in a 20–50 μs wide pulse at a controlled energy into a 7.6 cm long drift tube containing He buffer gas. The clusters exiting the drift tube are mass selected one more time and detected by an off-axis collision node and dual microchannel plates. The drift tube temperature and dual microchannel plates. The drift tube temperature was 300 K, the drift field was 15.5 V/cm, and the buffer gas pressure was between 6 and 10 Torr. The injection energy has been varied in the range of 190–390 eV, without a noticeable influence on the results.

The measured mobilities are plotted in Fig. 1, along with the data for Si [11], Ge [12], and Sn [18]

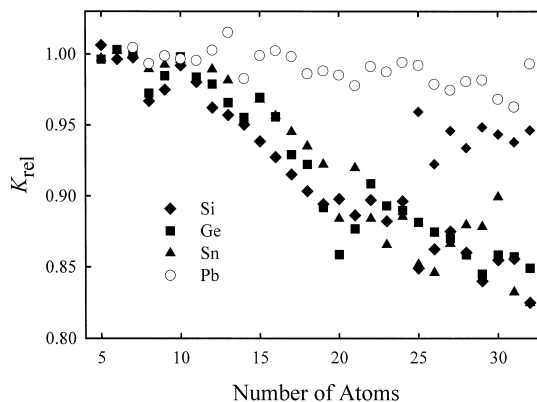


Fig. 1. Relative mobilities of group-14 cluster cations in the $n \leq 32$ size range measured at room temperature. Filled symbols are for Si_n (diamonds), Ge_n (squares), and Sn_n (triangles). Empty circles are for lead clusters.

cluster cations at room temperature. Only one feature was resolved for each size. All results are presented in terms of relative mobilities $K_{\text{rel}} = K_{\text{exp}}/K_{\text{sph}}$. Here K_{exp} is the mobility measured for an n -atom cluster and K_{sph} is that computed for a hypothetical sphere of a volume nV_{at} , where V_{at} is the atomic volume of the bulk element under ambient conditions. This normalization effectively cancels the systematic variation in mobility with cluster size, thus emphasizing the evolution of cluster shape as a function of number of atoms. Compact near-spherical isomers have larger relative mobilities, whereas smaller values indicate geometries that deviate substantially from spherical. The structural transition of Si_n cations from stacks of tricapped trigonal prisms to cage-like near-spherical geometries starting at $n = 25$ is apparent in Fig. 1. As described above, the mobilities of Ge_n and Sn_n cations in the $n \approx 10$ –35 range follow the global trend of prolate Si_n^+ , although some size-specific features for $n \geq 15$ are not identical. The behavior of lead clusters is clearly very different. Their relative mobilities decrease with increasing n only slightly. This decrease is not structurally related, but caused by multiple scattering. This effect decreases the mobility of any polyatomic ion, but its magnitude is always larger for larger sizes. An analogous gradual decrease in relative mobilities with increasing n has been observed for Si_n and Ge_n cations after the structural transition to near-spherical morphologies [18]. Thus Pb_n^+ species remain close-packed and near-spherical over the whole size range studied. This growth pattern is standard for the clusters of typical metals.

Two other findings are worthy of mention. First, the relative mobility of Pb_{13}^+ exceeds that of any other cluster in the studied size range, while Pb_{14}^+ exhibits a significant local minimum. This is consistent with the icosahedral packing, where the smallest perfect (Mackay) icosahedron can be assembled from 13 atoms. In comparison, the data for Si, Ge, and Sn cations do not show the maximum/minimum feature for $n = 13$ and 14. Second, the relative mobilities of Pb_n^+ in the $n = 25$ –32 range are systematically greater than those of Si_n^+ geometries after the structural transition. This appears to be the case because Pb clusters are densely packed, while the near-spherical Si_n species are cage-like with small empty spaces inside.

3. Conclusions

In summary, we have used ion mobility measurements to characterize the structure of gas-phase lead cluster cations with up to 32 atoms. For all sizes studied, these species have compact near-spherical geometries expected for normal metal clusters, with some indications for the icosahedral growth pattern. This means that the transition from covalent to metallic bonding in group-14 element clusters takes place between tin and lead. This conclusion is in agreement with the results of photoelectron spectroscopy studies [27,28].

Acknowledgements

We thank Dr. L. Molina and B. Wang for providing us their optimized geometries of some lead clusters. This research was supported by the National Science Foundation and the US Army Research Office.

References

- [1] W.A. de Heer, Rev. Mod. Phys. 65 (1993) 611.
- [2] E.K. Parks, B.J. Winter, T.D. Klots, S.J. Riley, J. Chem. Phys. 96 (1992) 8267.
- [3] M.F. Jarrold, J.E. Bower, J. Chem. Phys. 98 (1993) 2399.
- [4] M. Pellarin, B. Bagueard, C. Bordas, M. Broyer, J. Lerme, J.L. Vialle, Phys. Rev. B 48 (1993) 17645.
- [5] M. Pellarin, B. Bagueard, C. Bordas, M. Broyer, J. Lerme, J.L. Vialle, Z. Phys. D 26 (1993) S137.
- [6] K. Rademann, M. Ruppel, B. Kaiser, Ber. Bunsenges. Phys. Chem. 96 (1992) 1204.
- [7] G. Ganteför, S. Hunsicker, R.O. Jones, Chem. Phys. Lett. 236 (1995) 43.
- [8] A. Benamar, D. Rayane, P. Melinon, B. Tribollet, M. Broyer, Z. Phys. D 19 (1991) 237.
- [9] A. Ricca, C.W. Bauschlicher Jr., Chem. Phys. 208 (1996) 233.
- [10] G. von Helden, M.T. Hsu, N. Gotts, M.T. Bowers, J. Phys. Chem. 97 (1993) 8182.
- [11] M.F. Jarrold, V.A. Constant, Phys. Rev. Lett. 67 (1991) 2994.
- [12] J.M. Hunter, J.L. Fye, M.F. Jarrold, J.E. Bower, Phys. Rev. Lett. 73 (1994) 2063.
- [13] A.A. Shvartsburg, R.R. Hudgins, R. Gutierrez, G. Jungnickel, T. Frauenheim, K.A. Jackson, M.F. Jarrold, J. Phys. Chem. A 103 (1999) 5275.
- [14] Ph. Dugourd, R.R. Hudgins, J.M. Tenenbaum, M.F. Jarrold, Phys. Rev. Lett. 80 (1998) 4197.

- [15] K.M. Ho, A.A. Shvartsburg, B. Pan, Z.Y. Lu, C.Z. Wang, J.G. Wacker, J.L. Fye, M.F. Jarrold, *Nature (London)* 392 (1998) 582.
- [16] B. Liu, Z.Y. Lu, B. Pan, C.Z. Wang, K.M. Ho, A.A. Shvartsburg, M.F. Jarrold, *J. Chem. Phys.* 109 (1998) 9401.
- [17] A.A. Shvartsburg, B. Liu, Z.Y. Lu, C.Z. Wang, M.F. Jarrold, K.M. Ho, *Phys. Rev. Lett.* 83 (1999) 2167.
- [18] A.A. Shvartsburg, M.F. Jarrold, *Phys. Rev. A* 60 (1999) 1235.
- [19] J. Mühlbach, P. Pfau, K. Sattler, E. Recknagel, *Z. Phys. B* 47 (1982) 233.
- [20] J. Mühlbach, K. Sattler, P. Pfau, E. Recknagel, *Phys. Lett. A* 87 (1982) 415.
- [21] K. LaiHing, R.G. Wheeler, W.L. Wilson, M.A. Duncan, *J. Chem. Phys.* 87 (1987) 3401.
- [22] R.W. Farley, P. Ziemann, A.W. Castleman Jr., *Z. Phys. D* 14 (1989) 353.
- [23] A. Hoareau, P. Mélinon, B. Cabaud, D. Rayane, B. Tribollet, M. Broyer, *Chem. Phys. Lett.* 143 (1988) 602.
- [24] J.C. Phillips, *J. Chem. Phys.* 87 (1987) 1712.
- [25] Y. Saito, T. Noda, *Z. Phys. D* 12 (1989) 225.
- [26] T.P. Martin, H. Schaber, *J. Chem. Phys.* 83 (1985) 855.
- [27] G. Gantefor, M. Gausa, K.H. Meiwes-Broer, H.O. Lutz, *Z. Phys. D* 12 (1989) 405.
- [28] Ch. Lüder, K.H. Meiwes-Broer, *Chem. Phys. Lett.* 294 (1998) 391.
- [29] I. Rabin, W. Schulze, B. Winter, *Phys. Rev. B* 40 (1989) 10282.
- [30] R.W. Farley, P.J. Ziemann, R.G. Keesee, A.W. Castleman Jr., *Z. Phys. D* 25 (1993) 267.
- [31] X. Ren, K.M. Ervin, *Chem. Phys. Lett.* 198 (1992) 229.
- [32] D. Dai, K. Balasubramanian, *J. Chem. Phys.* 96 (1992) 8345.
- [33] D. Dai, K. Balasubramanian, *Chem. Phys. Lett.* 271 (1997) 118.
- [34] B. Wang, L.M. Molina, M.J. Lopez, A. Rubio, J.A. Alonso, M.J. Stott, *Ann. Phys.* 107 (1998) 7.
- [35] A.M. Mazzone, *Phys. Rev. B* 54 (1996) 5970.